Simulation of Visible Light Induced Effects in a Tunnel Junction Array for Photonic Device Applications

1999 Jpn. J. Appl. Phys. 38 593

(http://iopscience.iop.org/1347-4065/38/1S/593)

Jpn. J. Appl. Phys. Vol. 38 (1999) pp. 593–596
Part 1, No. 1B, January 1999

Simulation of Visible Light Induced Effects in a Tunnel Junction Array for Photonic Device Applications

Michiharu TABE, Yoichi TERAO, Ratno NURYADI, Yasuhiko ISHIKAWA, Noboru ASAHI[1] and Yoshihito AMEMIYA[1]

Research Institute of Electronics, Shizuoka University, 3-5-1 Johoku, Hamamatsu 432-8011, Japan
[1]*Faculty of Engineering, Hokkaido University, North 13 West 8, Sapporo 060-8628, Japan*

(Received June 1, 1998; accepted for publication August 28, 1998)

We have studied visible light or near-infrared irradiation effects in voltage-biased tunnel junction arrays, where each node is connected not only to neighboring nodes but to a conducting substrate through a tunnel barrier. Major assumptions used in the simulation are: (i) that the photoexcitation of electrons occurs only in the substrate and (ii) the tunnel barrier is effectively lowered for the excited electrons, resulting in a reduced tunnel resistance. As a result, it was found that a U-shaped potential profile is formed by local irradiation and the potential of the irradiated area is clamped at the lowest value. Since the currents at both terminals reflect the left and the right potential slopes in the dark areas, respectively, the irradiated position is determined by measuring the currents. These results suggest that tunnel junction arrays can be applied to photonic devices such as position sensing detectors or image processing devices.

KEYWORDS: tunnel junction array, photonic device, single electron tunneling, photon-assisted tunneling, visible light irradiation

1. Introduction

Single electron tunnel (SET) junction arrays are important in developing novel parallel-processing systems[1)] and analog computing systems using characteristic charge transport phenomena.[2,3)] Photonic devices using an SET transistor or a tunnel junction array are also fascinating because interactions with photons may lead to highly sensitive photosensors or image processing devices.[4–6)] Recently, microwave or far-infrared photon-assisted tunneling (PAT) has been intensively studied for single-dot and coupled-quantum dot structures.[7–10)] Kouwenhoven *et al*. studied microwave irradiation effects for a single-dot transistor structure,[8)] where 19-GHz microwaves are designed to generate an oscillating potential of the dot to the source and drain leads. They found that observed current-voltage characteristics follow a simple formula of the tunnel rate, an extension of the Tien-Gordon theory[11)] involving a modulated density of states. According to their formula, the tunnel rate is modulated by irradiation only in terms of a free energy difference between energies before and after SET, but the tunnel resistance is assumed unchanged, because the effective tunnel barrier height for photoexcited electrons is reduced only by a negligible amount ($h\nu = \sim 80\,\mu$eV).

On the other hand, PAT with a visible or near-infrared light ($h\nu$ = about 1–3 eV) has not been studied except for a few exceptions,[4,5)] although this shorter wavelength range is important in applications for image sensing and processing. In most practical junctions with relatively low tunnel barriers, electrons will be readily excited by such high energy photons beyond the tunnel barriers and move freely through junctions without Coulomb blockade restriction. Such situations are not of practical use, because characteristics of SET cannot be utilized in devices. Therefore, for excited electrons, the height of the effective tunnel barrier must be finite and the corresponding tunnel resistance must be larger than the resistance quantum $R_Q (= h/e^2)$. An n^+-Si/SiO_2 system, for example, has a tunnel barrier as high as 3.2 eV in the dark, where it is expected that the Coulomb blockade regime still holds under irradiation of the visible or near-infrared light.

In this study, we have modeled a layered structure, as an extension of our previous work,[6)] consisting of a one-dimensional (1D) or two-dimensional (2D) tunnel junction array on a thin insulating layer/a conducting substrate, and have studied local irradiation effects of a visible light on the potential profile and the circuit current. Although our results are not restricted to specific materials, a system with a high tunnel barrier such as a Si/SiO_2 system is implicitly required. Photo-induced reduction of the tunnel resistance is most important for a visible light in estimating tunnel rates, in contrast to a longer wavelength light, because the tunnel resistance for photoexcited electrons will be significantly reduced by several orders of magnitude. (Also, a shift of the circuit free energy by $h\nu$ is incorporated in some calculations. This effect, however, only serves to change the potential in the irradiated area.) As a result, it will be shown that characteristic charge and potential profiles are formed by irradiation and that the irradiated area is known from the potential profile or circuit currents measured at terminals.

2. Simulation Model

A 1D voltage-biased circuit is considered and is shown in Fig. 1(a), where 20 tunnel junctions (19 nodes) with C of 100 aF and R of 1 MΩ are connected in a series and each node is connected to the ground (substrate) via a tunnel junction with C_0 of 1 aF and R_0 of 100 MΩ. These values of tunnel resistances are defined as those in the dark. The bias voltage at both ends is chosen to be 500 mV. Circuit currents will be measured at the left and the right terminals, if necessary. Then, a visible light beam with a small spot diameter is locally illuminated onto five nodes, as shown in Fig. 1(b). It is assumed that photoabsorption occurs only in the substrate, because each node is, in practice, too thin and too small to absorb the light. Since photoexcited electrons in the substrate feel a reduced height of tunnel barrier towards overlying nodes, the tunnel resistance from the substrate to the nodes is reduced from R_0 to R_{ph} in the irradiated area. Here, it is also hypothesized that exited electrons after tunneling from the substrate to the dots quickly release their energy and that they have no chance to tunnel back to the substrate without relaxation. Therefore, the tunnel resistance from the nodes to the substrate remains R_0 even in the irradiated area. R_{ph} is assumed to be 100 kΩ, which is smaller than R_0 by three

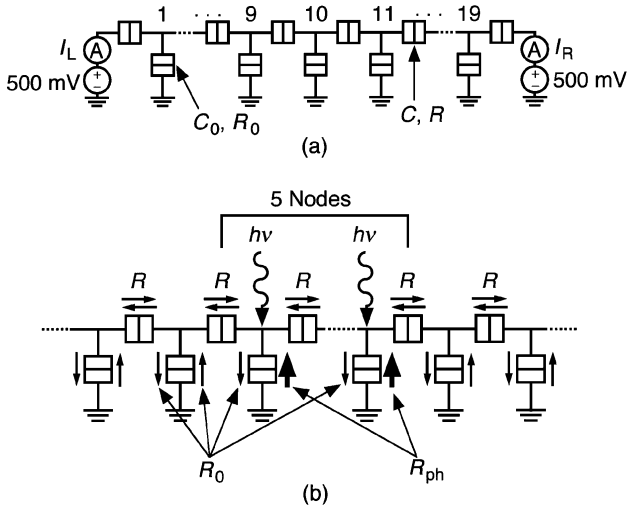

Fig. 1. (a) Equivalent circuit of a 1D voltage-biased array structure with 20 tunnel junctions (19 nodes). Each node is connected to the ground (substrate) via a tunnel junction. (b) Model for local irradiation of a visible light. In the simulation, the visible light is illuminated onto five nodes.

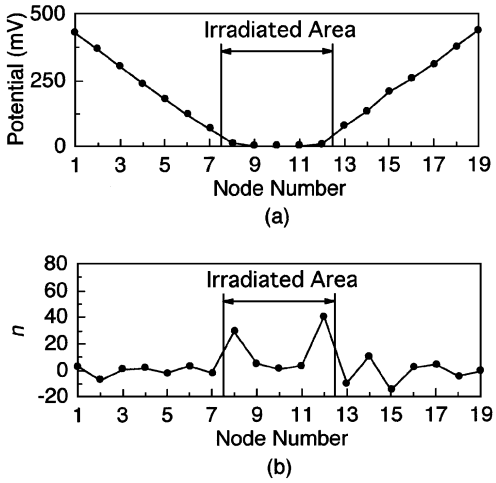

Fig. 2. Steady-state snapshots of (a) potential profile and (b) corresponding distribution of the number of electrons, n.

orders of magnitude but larger than R_Q. Unexcited electrons in the substrate, which also exist as well as excited electrons, are ignored in tunneling because of the high resistance.

In this calculation, we employed a Monte Carlo method using eq. (1) as a tunnel rate across junctions from the substrate to nodes in the dark area, from a node to a node and from a node to the substrate in both the dark and the irradiated areas, while eq. (2) is used only from the substrate to nodes in the irradiated area. The calculation procedure is the same as in our previous work.[3,6] For simplicity, the temperature is set to be 0 K, since even for finite temperatures the results are qualitatively the same for sufficiently small C and C_0.

$$\Gamma = \frac{1}{e^2 R_T} \frac{\Delta E}{[1 - \exp(-\Delta E/kT)]}, \quad (1)$$

$$\Gamma = \frac{1}{e^2 R_{ph}} \frac{\Delta E}{[1 - \exp(-\Delta E/kT)]}. \quad (2)$$

Here, R_T represents a tunnel resistance, R or R_0, and ΔE is a change in total free energy due to a tunnel event. In eq. (2), we have taken account of only a reduced tunnel resistance as an irradiation effect. However, in SET of an excited electron, not only a resistance reduction but a free energy shift will be involved. Therefore, in a more rigorous treatment, eq. (2) should be replaced by eq. (3) incorporating a photon energy shift, analogous to the formula by Kouwenhoven *et al.*[8] In eq. (3), ΔE is defined as a free energy change by tunneling without irradiation, and a single photon energy is added to ΔE. It will be shown later, however, that the effect does not qualitatively alter the results, and, therefore, we employed eq. (2) for the sake of simplicity in most of the present calculations.

$$\Gamma = \frac{1}{e^2 R_{ph}} \frac{\Delta E + h\nu}{\{1 - \exp[-(\Delta E + h\nu)/kT]\}}. \quad (3)$$

3. Results and Discussion

Steady-state snapshots of a potential profile and a corresponding charge (number of electrons, n) distribution are shown in Figs. 2(a) and 2(b), respectively, when five middle nodes (Node 8–Node 12) are irradiated. It is obvious from Fig. 2(a) that the potential in the irradiated area is clamped approximately at the ground and that the symmetrical potential slopes (electric fields) are formed in the left and the right dark regions. In Fig. 2(b), charge bumps are found at the edges of the irradiated area, while charges fluctuate around $n = 0$ at other nodes. Comparing the result in Fig. 2(a) with that in Fig. 2(b), we can see that the left (right) charge bump serves to screen an electric field caused by the left (right) voltage source. The origin of the charge bumps is interpreted as follows. In the irradiated area, excited electrons readily tunnel from the substrate to the overlying nodes. However, since the node-to-node resistance R is much higher than R_{ph}, electrons in the substrate preferentially tunnel to the left and right edge nodes in the irradiated area and subsequently flow to the left and right terminals, resulting in left and right current loops.

When the irradiated area is shifted towards the left (Node 4–Node 8) from the central position, the potential profile and the charge distribution are changed, as shown in Figs. 3(a) and 3(b), respectively. The potential in the irradiated area is again clamped at the ground, and therefore, the potential slopes, S_L and S_R, become different from each other. In Fig. 3(b), the charge bump at the right edge is smaller than that at the left edge, because the necessary amount of charge to screen the weaker electric field on the right is smaller. Figures 2 and 3 suggest that the irradiated area can be determined, if the resultant potential profile is measured using a scanning probe microscopy or other state-of-the-art techniques. This idea may be, however, impractical in device applications, so it is desired to find a more practical method, as described below.

The circuit currents, I_L and I_R, measured at the left and the right terminals, are plotted in Fig. 4 as a function of potential slope (electric field) S. For this calculation, the light spot is successively shifted from the central position towards the left terminal, i.e., S_L increases quickly and S_R decreases slowly, and the current is plotted without distinction between L and R. It is seen that the current depends almost linearly on the slope S. This result suggests a simple and practical method to detect the irradiated position; when the light spot is located at an asymmetric position, I_L and I_R are different from each other, and thus, the light-spot-position (more exactly, the left

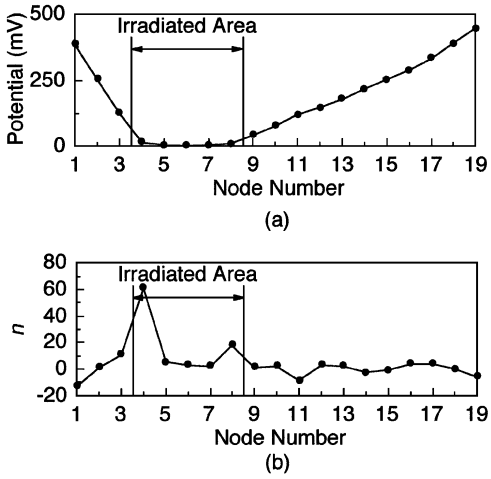

Fig. 3. (a) Potential profile and (b) charge distribution when the irradiated area is shifted towards the left (Node 4–Node 8).

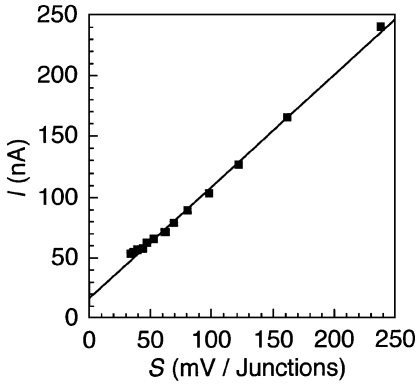

Fig. 4. Circuit current, I, as a function of potential slope, S.

and right edges of the irradiated area) can be determined by detecting I_L and I_R. In fact, I_L and I_R are 65 nA in Fig. 2, while $I_L = 120$ nA and $I_R = 55$ nA in Fig. 3.

These results can be extended to a 2D system. Figure 5 shows an example of a 2D system (7×7 nodes), where four terminals are equipped with voltage sources and current meters. It is assumed again that all nodes lie on the substrate at the ground potential via a tunnel barrier and that all parameter values are the same as those used in the 1D system. The irradiated area (3×3 nodes) is assumed to be at an asymmetric position, as indicated by the shaded area in Fig. 5. The potential profile and the charge distribution are plotted in Figs. 6(a) and 6(b), respectively. The potential in the irradiated area is flat and clamped at the ground as in the 1D system. Four terminal currents (I_L, I_R, I_U and I_D) are found to be 990 nA, 400 nA, 940 nA and 410 nA, respectively, while the currents are found to be equal to each other (620–640 nA) when the irradiated area lies at the central position of the 2D array. Therefore, the spot area can be determined from these values; a larger value of I_L than that of I_R and a larger value of I_U than that of I_D indicate that the irradiated area deviates to an upper left position.

Finally, we have examined the effect of a photon energy shift in ΔE, as expressed in eq. (3), for $h\nu$ of 2 eV. The results are shown in Figs. 7(a) and 7(b), when we calculate PAT using eq. (3) in a similar situation as in Fig. 1. It was found

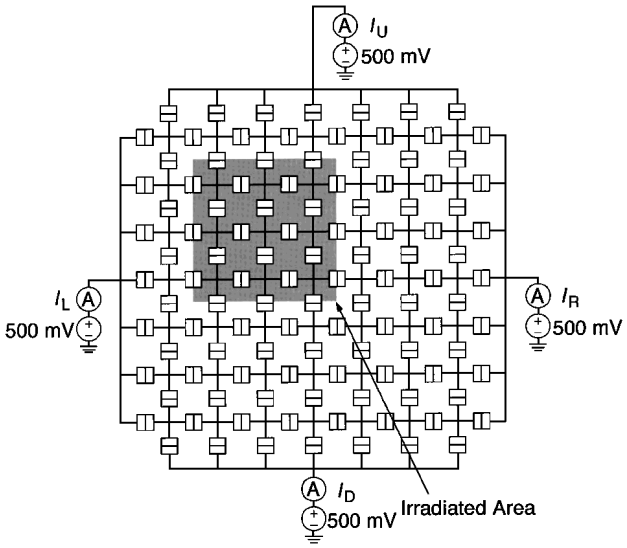

Fig. 5. Equivalent circuit of 2D voltage-biased array structure (7×7 nodes). Each node is connected to the ground (substrate) via a tunnel junction. Irradiated area (3×3 nodes) is indicated by the shaded area.

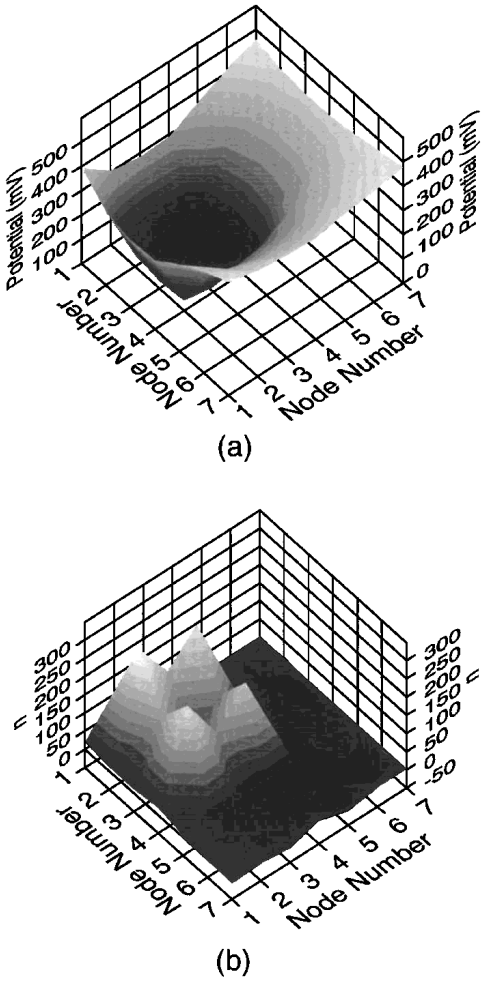

Fig. 6. (a) Potential profile and (b) charge distribution for the 2D system shown in Fig. 5.

that the most prominent difference observed from Fig. 2 is the potential in the irradiated area, i.e., the potential is not at the ground but biased by -2 V. This result implies that the

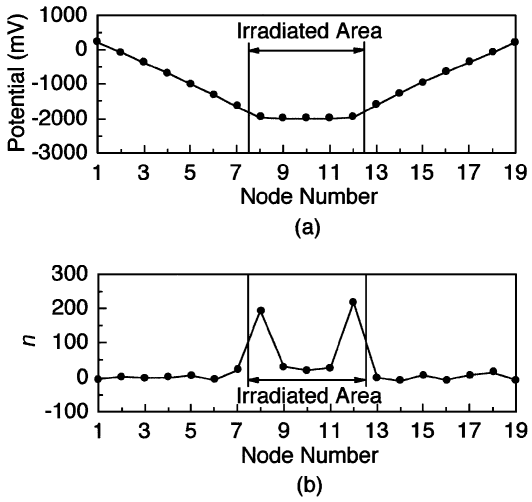

Fig. 7. (a) Potential profile and (b) charge distribution for the 1D system (Fig. 1), taking account of the effect of a photon energy shift in ΔE.

Coulomb blockade threshold is shifted by $h\nu/e$ and electrons are pumped from the substrate to the nodes in the irradiated area. However, the effect of the resistance reduction on tunnel rates is much larger than that of the energy shift, because the resistance is reduced by several orders of magnitude, *e.g.*, three orders in this work, but the free energy is shifted only by $h\nu$ which is almost of the same order as a typical value of ΔE.

These results suggest that a 1D or a 2D tunnel junction array works as a spot position sensor by measuring the potential profile or, more practically, measuring the terminal currents, which may be extended to image processing devices. Although a local irradiation with a small spot size was considered in this work, for a larger light spot covering the entire array, the photocurrent should be the highest and the array simply acts as a photodetector.

4. Conclusion

We have studied photoirradiation effects by Monte Carlo simulation in voltage-biased 1D and 2D tunnel junction arrays lying on a conducting substrate through a tunnel barrier. It is assumed that photoexcitation of electrons occurs only in the substrate and the excited electrons tunnel with a small resistance. The results showed formation of a U-shaped potential profile, in which the irradiated area was clamped at the lowest potential. Since the currents at both terminals reflect the left and the right potential slopes, respectively, the irradiated area is determined by measuring these currents or the potential profile. Therefore, it was suggested that tunnel junction arrays may be applied to photonic devices such as position sensing detectors or image processing devices.

Acknowledgment

This work is partly supported by a Grant-in-Aid for Scientific Research on Priority Area from the Ministry of Education, Science, Sports and Culture and by Takahashi Industrial and Economic Research Foundation.

1) P. D. Tougaw, C. S. Lent and W. Porod: J. Appl. Phys. **74** (1993) 3558.
2) K. K. Likharev, N. S. Bakhvalov, G. S. Kazacha and S. I. Serdyukova: IEEE Trans. Magn. **25** (1989) 1436.
3) M. Tabe, N. Asahi, Y. Amemiya and Y Terao: Jpn. J. Appl. Phys. **36** (1997) 4176.
4) A. N. Cleland, D. Esteve, C. Urbina and M. H. Devoret: Appl. Phys. Lett. **61** (1992) 2820.
5) A. Fujiwara, Y. Takahashi and K. Murase: Phys. Rev. Lett. **78** (1997) 1532.
6) M. Tabe, Y. Terao, N. Asahi and Y. Amemiya: IEICE Trans. Electron. **E81-C** (1998) 36.
7) P. Delsing, K. K. Likharev, L. S. Kuzmin and T. Claeson: Phys. Rev. Lett. **63** (1989) 1861.
8) L. P. Kouwenhoven, S. Jauhar, K. McCormick, D. Dixon, P. L. McEuen, Yu. V. Nazarov, N. C. van der Vaart and C. T. Foxon: Phys. Rev. B **50** (1994) 2019.
9) C. Bruder and H. Schoeller: Phys. Rev. Lett. **72** (1994) 1076.
10) M. Wagner and W. Zwerger: Phys. Rev. B **55** (1997) R10217.
11) P. K. Tien and J. P. Gordon: Phys. Rev. **129** (1963) 647.